Supporting Information

Karagiannis and Popel 10.1073/pnas.0803241105

SI Materials and Methods

Computational Analysis. Multiple sequence alignments and the clustering dendrogram of the amino-acid sequences were performed by using the ClustalW algorithm (1). A custom based bioinformatics algorithm was used to search for similarities of the known antiangiogenic peptides within the human proteome.

Bioinformatics Algorithm. To identify the conserved domains present within the queries, the National Center for Biotechnology Information's (NCBI) conserved domain database (CDD) search option (2) was used as part of the protein BLAST algorithm. Along with the NCBI's CDD search, the European Molecular Biology Laboratory's (EMBL) simple modular architecture research tool (3) sequence analysis algorithm was also used to identify conserved domains. Information for each of the hits, considering their localization as well as basic function, was collected using the EMBL's Harvester database (4). In the case of proteins with known active domains and lengths $<$150 aa, the total protein sequence was used to identify a conserved domain and not just the fragment. Subsequently, the active domains were localized within the query and classified as to whether they belonged to or included specific conserved domains.

For sequence similarity searches, NCBI's basic local alignment search tool for proteins (BLASTp) algorithm was used. Each search was performed for human proteins using the default options of the algorithm, except that the expectation value was increased from 10 to 1000 and the word size was decreased from 3 to 2. These modifications were made because the small length of some queries (15–20 aa) made it probable that results calculated by using these low-level criteria might be significant and therefore should not be rejected *ab initio*. Proteins with significant similarities were initially identified by using these low-level criteria. For each of the queries, ≈1000 initial similar hits were identified.

To ascertain whether the identified proteins were truly similar or whether they had been selected erroneously because of the low-level search criteria, we used a Monte-Carlo-type algorithm to filter the initial hits once we had considered the E values of the results as provided by BLASTp. Given that these hits were found using the BLASTp search, there was some evidence for similarity between the query and the hit. It was therefore reasonable to expect that the score for the alignment of a truly similar BLASTp hit with the initial query would be higher than the scores obtained by aligning a random sequence of amino acids with this same BLASTp hit.

By conserving the amino-acid composition of the initial query, i.e., the original antiangiogenic protein or fragment, and after randomly permuting the amino-acid locations, we created a set of 100 new random sequences for each of the queries. The similarity of each of these 100 artificial sequences to each of the initial BLASTp hits was calculated and the resulting scores were fitted to an extreme value distribution probability density function. This distribution describes the probability that the alignment score is random, rather than a significant hit. The scores for the original protein's local alignment with each of the BLASTp hits were superimposed on the scores of each of the random sequences, and only those greater than the scores for the random sequences were retained.

Local alignments were performed with the Smith-Waterman algorithm by using the BLOSUM 50 substitution matrix as the scoring matrix. The BLOSUM 50 matrix identifies highly similar proteins that are likely to share similar overall structure, regardless of whether they have distant evolutionary origins or are closely related sequences (5). The resulting score for each alignment, in bits, was scaled by using the score of the alignment of the initial query with itself as a scaling factor. We considered a scaled score $>$40% a threshold for similarity. All of the algorithms were implemented in Matlab (Mathworks).

Peptide Synthesis and Handling. The peptides were produced by a commercial provider (Abgent) using a solid phase synthesis technique. HPLC and MS analyses of each peptide were performed. In each case, the synthetic procedure yielded $>$95% pure peptide. In the cases of highly hydrophobic peptides, DMSO at a maximum concentration of 0.1% (vol/vol) was used as a solvent; we verified experimentally that at this concentration, the solvent had no effect on the experimental results.

Cell Culture. Primary human umbilical vein endothelial cells (HUVECs) from a single donor were purchased from Cambrex. The cells were propagated in EGM-2 medium, consisting of a basal cell medium with 2% FBS, growth factors human basic FGF and VEGF, and antibiotics (gentamicin/amphotericin B). All of the cells used were from passages 3- 6.

***In Vitro* Cell Viability and Migration Assays.** In vitro *cell viability assay.* A commonly used way to assess the effects of an antiangiogenic agent on the proliferation of endothelial cells is to monitor the viability and metabolic activity of the cells in the presence of the agent at different concentrations after various periods of time. We used the colorimetric cell proliferation reagent WST-1 (4-[3-(4-iodophenyl)-2-(4-nitrophenyl)-2H-5-tetrazolio]-1,3-benzene disulphonate) (Roche) as the substrate in an assay that measures the metabolic activity of viable cells (6). The assay is based on the reduction of the red tetrazolium salt WST-1 by viable, metabolically active cells to form yellow formazan crystals that are soluble in the cell culture medium.

The cells were cultured as described above and then trypsinized and resuspended in EGM-2 once they had reached 80% confluence. Cell counts were determined using a hemocytometer.

The proliferation assay involved two steps. During the first step, the cells ($\approx 2 \times 10^3$ cells per well in a 96-well microplate) were seeded without any extracellular matrix substrate onto the microwells overnight (8 h). The initial cell culture medium was then removed, and the candidate peptides, dissolved in cell culture medium with growth factors and serum, were added to the wells. The viability of the cells was determined after a 3-day exposure to the peptide solution. Each peptide was tested at seven different concentrations: 0.01, 0.1, 1, 10, 20, 30, and 40 μg/ml. Each of the concentrations was tested simultaneously in quadruplicate, and each of the experiments was repeated two times. As a positive control (i.e., decreasing viability) we applied 100 ng/ml (0.22 μM) TNP-470 [O-(chloro-acetyl-carbamoyl) fumagillol, a synthetic analogue of fumagillin, 0.46 kDa, provided by the National Cancer Institute] along with the full medium. As a negative control (equivalent to normal viability), the cells were cultured without any agent in full medium containing growth factors and serum. The cells were then incubated with the WST-1 reagent for ≈3 h. During the incubation period, the mitochondria of viable cells convert the red WST-1 to yellow formazan crystals that dissolve in the medium. The second step of the assay involved the quantification of the changes in proliferation by measuring the changes in the color of

the metabolized substrate. The samples were read at a wavelength of 570 nm in a plate reader (Victor 3V, Perkin–Elmer). The amount of color produced was directly proportional to the number of viable cells.

In vitro *cell migration assay.* A modified Boyden chamber migration assay (BD Biosciences) was used to examine endothelial cell migration in the presence of an activator. The lower compartment of the Boyden chamber was separated from the upper (containing the endothelial cells) by a laminin-coated polycarbonate filter with pores small enough to allow only the active passage of the cells (3-μm pore size). Laminin was used as the extracellular matrix component for cell attachment and migration because it is considered to be the preferred substrate for testing the ability of the novel peptides to suppress the migration of endothelial cells during the angiogenic process. In this case, there was no need for matrix metalloproteinase (MMP) expression by the endothelial cells, which is required for invasion assays involving migration through a collagenous substrate. Furthermore, the expression of MMPs, which plays a major role in the invasion assay, may cause remodeling and degradation of the extracellular matrix components and release of cryptic fragments of the extracellular matrix other than those tested in the present study. Consequently, the use of laminin allowed us to minimize any potential interference from other unknown fragments and ensure that the migration assay mimicked a more basic activity of the endothelial cells (increasing in their motility), rather than the combination of migration and proteolytic activity that is characterized by the expression of MMPs in the invasion assay.

The cells were applied to the upper compartment of the chamber. Typically, 30×10^3 cells in a volume of 50 μl were added to each well. The growth factor VEGF (Invitrogen) was used as the activator. It was added to serum-free medium in the lower chamber to give a final concentration of 20 ng/ml in a total volume of 225 μl. VEGF in serum-free medium was also used alone as a positive control. The antiangiogenic peptides to be tested were individually added to the lower chamber at 30 μg/ml, together with 20 ng/ml VEGF in serum-free medium. The serum- and growth factor-free medium was used alone as a negative control. The chambers were then incubated for 20 h at 37°C; this period was sufficient to allow measurable numbers of cells to migrate through the filter. Each peptide was tested in eight wells per experiment, and each of the experiments was repeated in duplicate, in accordance with the manufacturer's instructions. After 20 h, the cell medium was removed, and the endothelial cells that migrated to the bottom part of the porous membrane were stained with calcein (Invitrogen) 90 min before termination of the experiment; this indicator is internalized by endothelial cells. The cells that had migrated into the lower chamber were counted by measuring the fluorescence at 485-nm excitation and 510-nm emission in a fluorescence plate reader (Victor 3V). The wells are fluorescence-impermeable; thus, only the fluorescence emission from cells that migrated into the lower chamber is measured. The intensity of the signal is directly proportional to the number of endothelial cells that are present in the lower chamber. The results were scaled so that the scale represents the percentage of migration inhibition. Here, 100% represents the negative control (serum- and growth-factor-free medium) with total migration inhibition, and 0% represents the positive control where we expect zero migration inhibition.

The results of these proliferation assays identified two distinct types of activity: one group of peptides, including all of the collagen-derived peptides, most of the TSP1 domain-containing protein-derived peptides (such as thrombostatin containing-6, properdistatin, wispostatin-2, nephroblastostatin, SCOspondinstatin, and connectostatin), and some of the chemokinostatins (-3 and -5), showed a typical monotonic dose response pattern of activity. The antiproliferative efficiency increased with escalating concentrations of the applied peptide, until saturation was reached. The second group consisted of some TSP1 repeat-containing protein-derived peptides, such as papilostatin, and semastatin-5B, as well as some chemokinostatins (-1, -6, and -7). These peptides exhibited a biphasic (nonmonotonic) response: Their activity reached a maximum at an intermediate concentration and decreased as the concentration was increased. This biphasic type of response in the *in vitro* proliferation assays is typical of endogenous peptide inhibitors of angiogenesis. Some characteristic examples of such biphasic responses include the antiproliferative effects of the full-length endostatin *in vitro* and *in vivo* (7, 8) and its small fragment derivatives (9), the antiangiogenic domains derived from the thrombospondin-1 and thrombospondin-2 proteins (10).

Statistical Analysis. Statistical significance was assessed by using the Student's *t*-test, with P values <0.001 defined as significant. The question being tested was whether the scaled experimental result was different from the negative control.

Monoclonal Antibody Neutralization Assay. In the monoclonal antibody neutralization experiments, 2,000 endothelial cells per well were seeded overnight in 96-well plates in full growth factor and serum medium. The medium was removed and replaced with medium containing different monoclonal antibody solutions for β1 integrins (R&D Systems FAB17781), $\alpha v\beta 3$ integrins (R&D Systems FAB3050), CXCR3 (R&D Systems FAB1685), CD36 (BD PharMingen CB38/NL07), and CD47 (BD PharMingen B6H12). The cells were incubated for 2 h with the antibody solutions. After the 2 h, the peptide solutions at different concentrations were added in the wells. As a control, a set of cells was incubated only in the presence of the monoclonal antibody solutions and without any peptides. The cells were incubated for 3 d, and the cell viability estimation was performed by using the colorimetric cell proliferation reagent WST-1 in a similar manner to the quantification performed in the proliferation assay.

Peptide Combination Assay. In the combination experiments, 2,000 cells per well were seeded in 96-well microplates. The cells were allowed to attach overnight in full growth factor and serum medium. The full medium was withdrawn, and a solution of a single peptide was applied in dose response concentrations of 0.1, 1, 10, and 30 μg/ml. These solutions were prepared and applied in growth-factor- and serum-free medium. After 2 h, the solutions of the first peptide were withdrawn and the solutions of the second peptide were applied in a growth-factor- and serum-free medium. The concentrations at which the second peptide was applied were the same as the concentrations of the first. In addition to the combinations, each of the peptides was applied alone for reference. After 24 h, the WST-1 dye was applied and the number of live cells was estimated by the optical signal. Dose responses were estimated by fitting the data to sigmoidal Hill curves.

Antibody Competition. In the antibody competition experiments, 10,000 endothelial cells per well were seeded overnight in 96-well plates in full growth factor and serum medium. The medium was removed and replaced with medium containing different peptide concentrations. After 2 h of incubation, the peptide solution was removed and the cells were fixed with 3.7% paraformaldehyde for 30 min. After washing with PBS, nonspecific binding sites were blocked by incubating the cells with 10% goat serum solution in PBS for 1 h at room temperature. Different monoclonal antibody solutions were prepared. The antibodies were tagged with different fluorescent tags. The antibody for β1 integrins was tagged with phycoerythrin (PE) (R&D Systems FAB 17781P), the CXCR3 antibody also with PE (R&D Systems FAB 160P), and the CD36 antibody with FITC (BD PharMingen

CB38/NL07). The cells were incubated for 1 h with the antibody solutions (0.5 μg/ml of β1 antibody, 1 μg/ml of CXCR3 antibody, and 50 ng/ml of CD36 antibody) at 4°C. The cells were washed and the fluorescence was measured by using a fluorescent plate reader (Victor 3V) using the factory designated excitation and emission wavelengths for the dyes.

Isobologram and Combination Index Calculation. In the combination proliferation experiments, the endothelial cells were incubated with different concentrations of two different peptides. After 1 d of peptide application, the cells were then incubated with the WST-1 reagent for ≈3 h. During the incubation period, the mitochondria of viable cells convert the red WST-1 to yellow formazan crystals that dissolve in the medium. The samples were read at a wavelength of 570 nm in a Victor 3V plate reader. The amount of color produced was directly proportional to the number of viable cells.

Dose response sigmoidal curves for a condition "i" were estimated by fitting the data to sigmoidal Hill curves of the type:

$$E_i = E_i^{max} \cdot \frac{D_i^{n_i}}{D_{50,i}^{n_i} + D_i^{n_i}} \rightarrow D_i = D_{50,i} \cdot \sqrt[n_i]{\frac{E_i}{E_i^{max} + E_i}} \quad [1]$$

where E is the effect of the condition "i", in this case, the fraction of dead cells; E^{max} is the maximum observed effect; D is the corresponding dose that yields effectiveness E; D_{50} is the dose at which half of the maximum effectiveness E^{max} is observed; and n is the Hill coefficient.

If we combine a peptide x with a peptide y and D_x^{combo} is the applied peptide x concentration in the combination experiment and D_y^{combo} is the applied peptide y concentration in combination, then because of the set up of the experiment, at each experimental condition $D_x^{combo} = D_y^{combo} = D^{combo}$. To construct an isobologram, a graph of equally effective dose pairs (isoboles) for a single peptide effect level (11), we consider:

$$\frac{D_x^{combo}}{D_x} + \frac{D_y^{combo}}{D_y} = 1 \quad [2]$$

In the denominator, D_x is the dose for D_x^{combo} alone that inhibits the proliferation by effectiveness E, and D_y is the dose for D_x^{combo} alone that inhibits the proliferation by the same effectiveness E. Also $D_x^{combo} = D_y^{combo} = D^{combo}$. Solving Eq. 2 for a single dose:

$$D_x = \frac{D_y \cdot D^{combo}}{D_y - D^{combo}} \quad [3]$$

After substituting the dose response of the combination D^{combo} with the corresponding sigmoidal Eq. 1 as fitted by the experimental data, Eq. 3 becomes:

$$D_x = \frac{D_y \cdot D_{50}^{combo} \cdot \sqrt[n_{combo}]{\frac{E_{combo}}{E_{combo}^{max} + E_{combo}}}}{D_y - D_{50}^{combo} \cdot \sqrt[n_{combo}]{\frac{E_{combo}}{E_{combo}^{max} + E_{combo}}}} \quad [4]$$

The isobologram is the plot of these concentrations that the effectiveness of an agent alone is the same as the effectiveness of the same agent in combination, $E_{combo} = E_y$, thus Eq. 4 becomes:

$$D_x = \frac{D_y \cdot D_{50}^{combo} \cdot \sqrt[n_{combo}]{\frac{E_y}{E_{combo}^{max} + E_y}}}{D_y - D_{50}^{combo} \cdot \sqrt[n_{combo}]{\frac{E_y}{E_{combo}^{max} + E_y}}} \quad [5]$$

But the effectiveness for y alone is defined according to the Hill equation as:

$$E_y = E_y^{max} \cdot \frac{D_y^{n_y}}{D_{50,y}^{n_y} + D_y^{n_y}} \quad [6]$$

Thus after substituting Eq. 6 into Eq. 5:

$$D_x = D_y \cdot D_{50}^{combo} \cdot \frac{\sqrt[n_{combo}]{\frac{E_y^{max} \cdot \frac{D_y^{n_y}}{D_{50,y}^{n_y} + D_y^{n_y}}}{E_{combo}^{max} + E_y^{max} \cdot \frac{D_y^{n_y}}{D_{50,y}^{n_y} + D_y^{n_y}}}}}{D_y - D_{50}^{combo} \cdot \sqrt[n_{combo}]{\frac{E_y^{max} \cdot \frac{D_y^{n_y}}{D_{50,y}^{n_y} + D_y^{n_y}}}{E_{combo}^{max} + E_y^{max} \cdot \frac{D_y^{n_y}}{D_{50,y}^{n_y} + D_y^{n_y}}}}} \quad [7]$$

To graph the isobolograms, we calculate the corresponding D_x for each D_y and plot the D_x vs. D_y pairs.

The isobolograms are a special case for the combination index equation as introduced by Chou and Talalay (12). The generic equation for the combination index calculation is expressed:

$$CI = \frac{D_x^{combo}}{D_x} + \frac{D_y^{combo}}{D_y} \quad [8]$$

If $CI < 1$, the drug combination effect is synergistic; if $CI = 1$, the drug combination effect is additive; whereas if $CI > 1$, the drug combination effect is antagonistic.

1. Thompson JD, Higgins DG, Gibson TJ (1994) CLUSTAL W: Improving the sensitivity of progressive multiple sequence alignment through sequence weighting, position-specific gap penalties and weight matrix choice. *Nucleic Acids Res* 22:4673–4680.
2. Marchler-Bauer A, Bryant SH (2004) CD-Search: Protein domain annotations on the fly. *Nucleic Acids Res* 32:W327–331.
3. Letunic I, *et al*. (2004) SMART 4.0: Towards genomic data integration. *Nucleic Acids Res* 32:D142–144.
4. Liebel U, Kindler B, Pepperkok R (2004) 'Harvester': A fast meta search engine of human protein resources. *Bioinformatics* 20:1962–1963.
5. Pearson, WR (2000) Flexible sequence similarity searching with the FASTA3 program package. *Methods Mol Biol* 132:185–219.
6. Ishiyama M, *et al*. (1996) A combined assay of cell viability and in vitro cytotoxicity with a highly water-soluble tetrazolium salt, neutral red and crystal violet. *Biol Pharm Bull* 19:1518–1520.
7. Celik I, *et al*. (2005) Therapeutic efficacy of endostatin exhibits a biphasic dose-response curve. *Cancer Res* 65:11044–11050.
8. O'Reilly MS, *et al*. (1997) Endostatin: An endogenous inhibitor of angiogenesis and tumor growth. *Cell* 88:277–285.
9. Tjin Tham Sjin RM, *et al*. (2005) A 27-amino-acid synthetic peptide corresponding to the NH2-terminal zinc-binding domain of endostatin is responsible for its antitumor activity. *Cancer Res* 65:3656–3663.
10. Tolsma SS, *et al*. (1993) Peptides derived from two separate domains of the matrix protein thrombospondin-1 have anti-angiogenic activity. *J Cell Biol* 122:497–511.
11. Chou TC (2006) Theoretical basis, experimental design, and computerized simulation of synergism and antagonism in drug combination studies. *Pharmacol Rev* 58:621–681.
12. Chou TC, Talalay P (1984) Quantitative analysis of dose-effect relationships: The combined effects of multiple drugs or enzyme inhibitors. *Adv Enzyme Regul* 22:27–55.

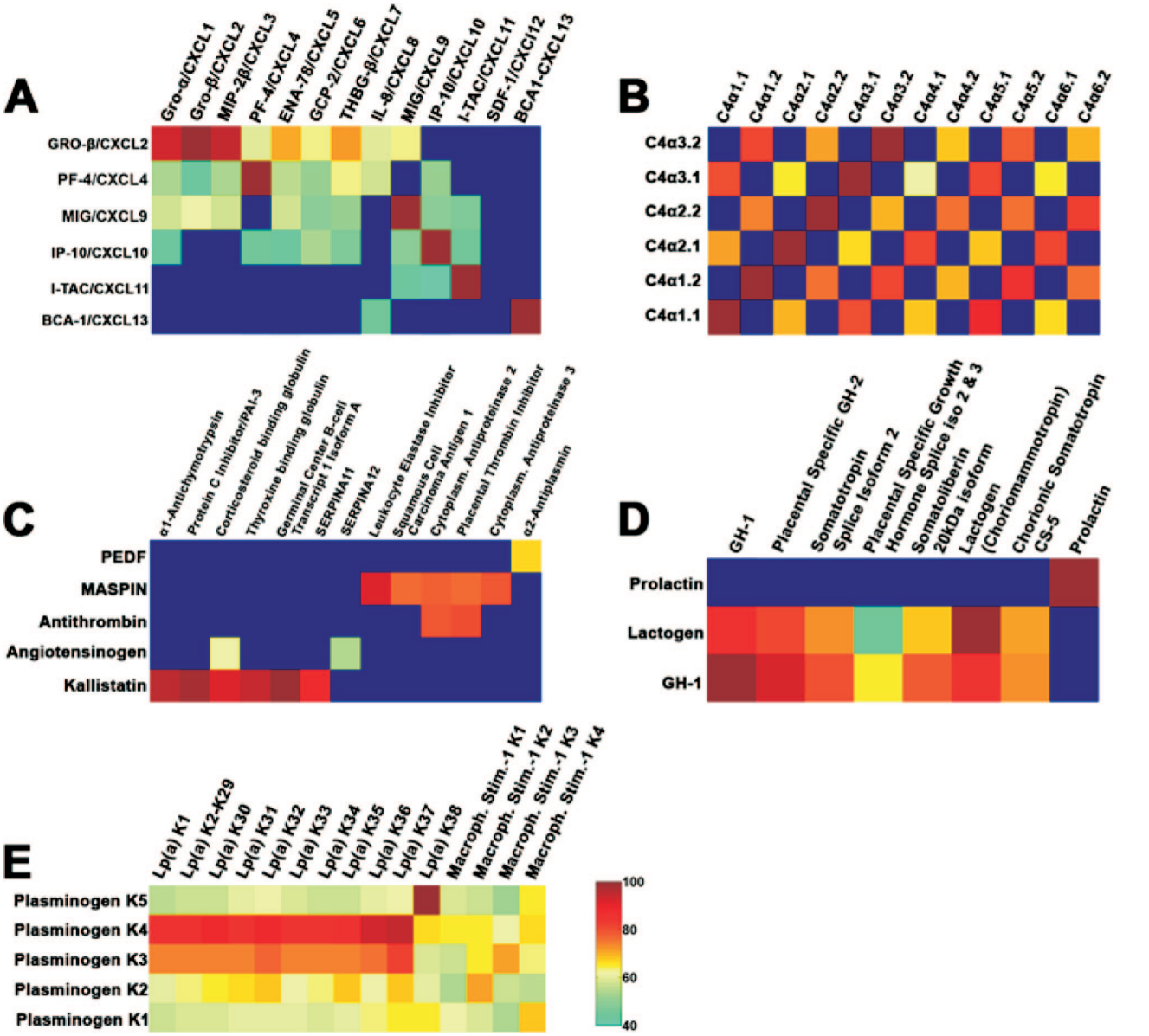

Fig. S1. Scaled similarity scores (bits) for different families of proteins classified based on the existence of a common conserved domain. (*A*) Proteins containing a CXC conserved domain. (*B*) Proteins that contain a collagen type IV domain. (*C*) Proteins that belong to the serpin family. (*D*) Kringle containing proteins. (*E*) Proteins with a somatotropin hormone conserved domain. As in Fig. 1, the similarity between the query (vertically positioned domain) and the corresponding domains of various proteins (horizontally positioned domains) is calculated. Similarities scoring >45% are color-coded, whereas lower scores are represented by the blue color.

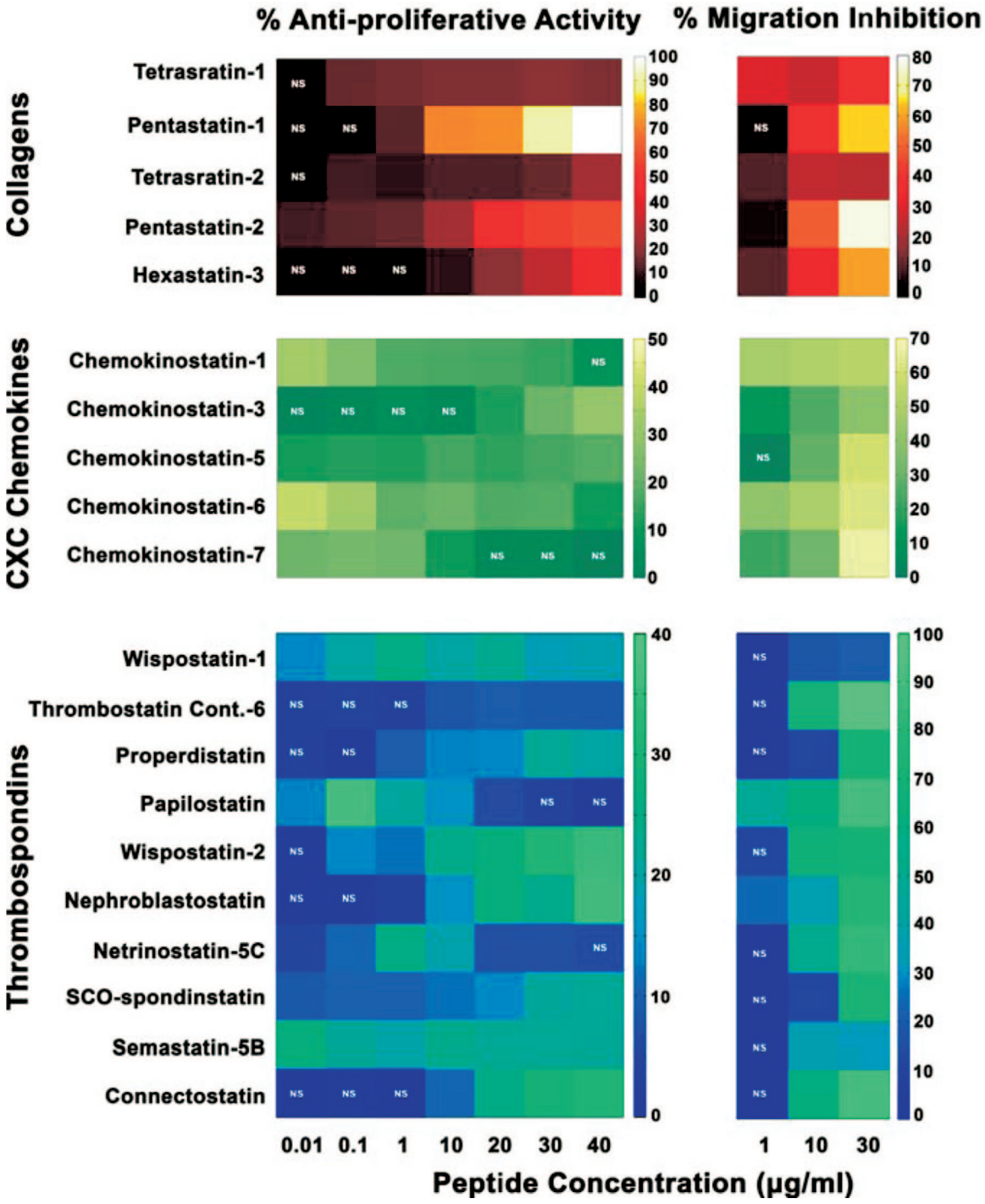

Fig. S2. Effect of 20 short peptides derived from collagen IV, CXC chemokines, and thrombospondin-1 repeat-containing proteins on the proliferation and migration of HUVECs. The results in these proliferation experiments were scaled so that 0% represents the number of cells from the negative control (endothelial cells incubated with medium containing growth factor and serum) (data not shown) and 100% represents the number of cells from the positive control (cells incubated with 100 ng/ml TNP-470) (data not shown). In the migration experiments, the effect of the same 20 peptides on the migration of HUVECs was evaluated in a modified Boyden chamber migration assay. The migrating cells were stained with calcein, and the fluorescent signal was scaled so that 0% represents the level of staining for the negative control (endothelial cells in serum- and growth-factor-free medium) (data not shown) and 100% the level of staining for the positive control (migration in the presence of 20 ng/ml VEGF) (data not shown). All values are significantly different from 0% at $P < 0.001$, except those marked by NS (nonsignificant). In all cases, the standard error was <4% ($n = 8$).

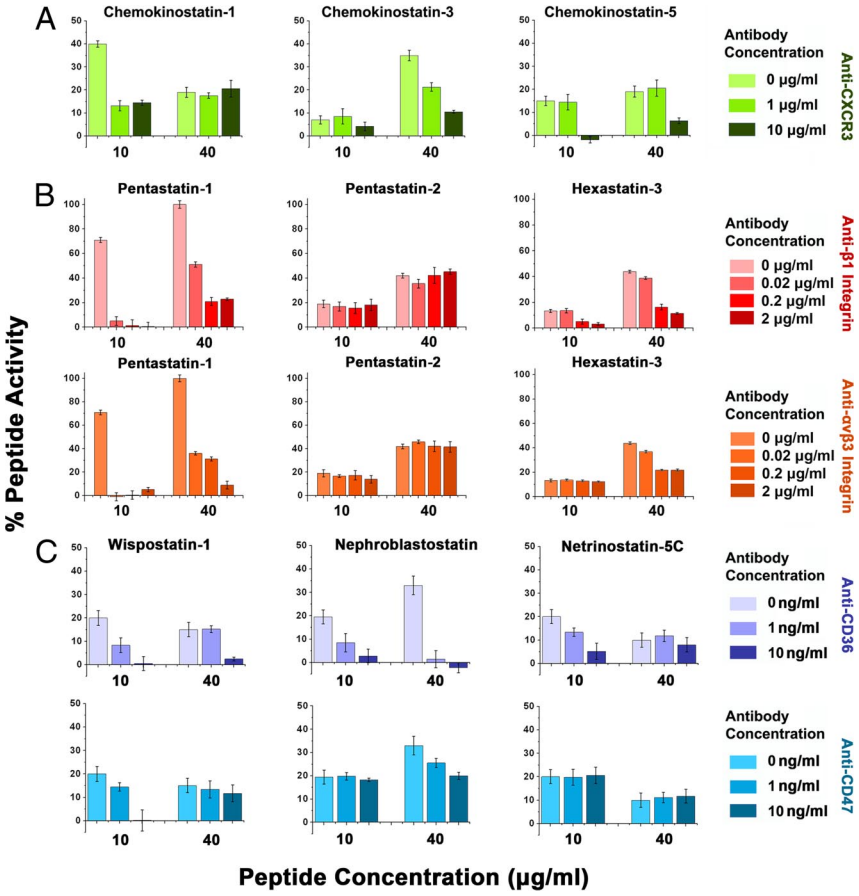

Fig. S3. Characterization of candidate receptors for the peptides. HUVEC proliferation assays were used to test the ability of peptides to inhibit proliferation after pretreatment of the cells with specific antibodies to neutralize various receptors associated with antiangiogenic activity. (*A*) The effect of two different concentrations of the CXCR3 receptor-neutralizing antibody on the activity of the CXC chemokine-derived peptides (green). (*B*) The effect of β1 and $\alpha v\beta 3$ integrin-neutralizing antibodies on the activity of the collagen IV-derived peptides pentastatin-1, pentastatin-2, and hexastatin-3 (red). (*C*) The effect of CD36 and CD47 receptor-neutralizing antibodies on the activity of thrombospondin-derived peptides (blue).

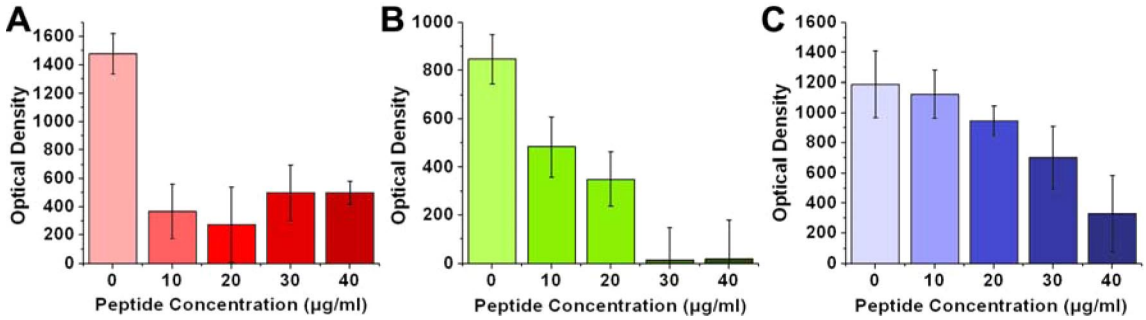

Fig. S4. Antibody competition assay for three major peptide receptors. (*A*) The competition assay for β1 integrins using pentastatin-1 and a PE tagged antibody. The cells were preincubated with varying concentrations of peptide for 2 h. The peptide solutions were removed, and the cells were fixed and stained with 0.5 μg/ml of anti-β1 antibody. After washing, the fluorescent signal was measured. In all of the tested concentrations, the peptide inhibited the antibody binding. Some signal in the assay can be attributed to nonspecific binding. (*B*) The competition assay for the CXC chemokine derived peptide, chemokinostatin-1. The assay was repeated with a PE tagged anti-CXCR3 antibody after incubating the cells with the peptide. The antibody was applied at 0.5 μg/ml concentration and the signal was measured after washing. (*C*) The competition assay for the TSP1 repeat-containing derived peptide properdistatin. An anti-CD36 antibody tagged with FITC was applied to the cells at 50 ng/ml after incubation with different peptide concentrations, and after washing, the optical signal was measured.

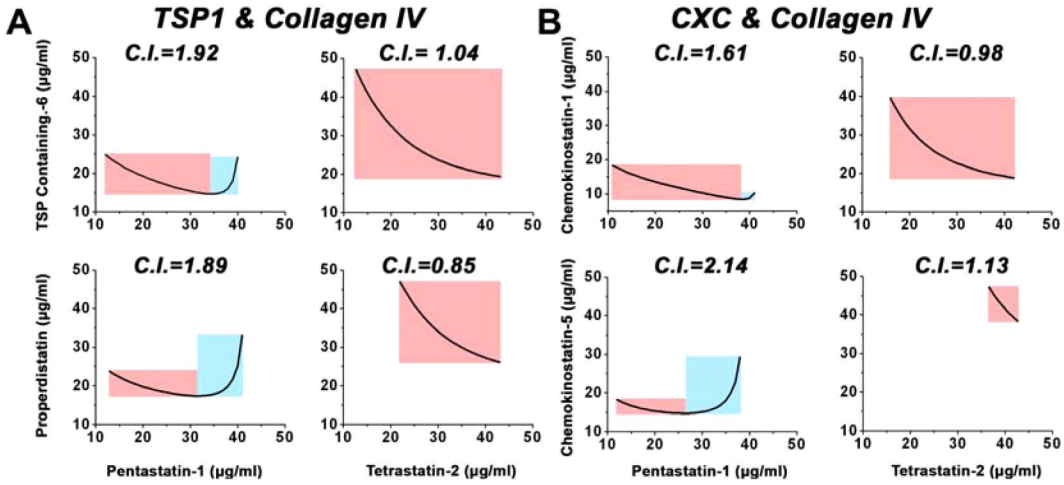

Fig. S5. Evaluation of peptide combinations derived from TSP1-containing, CXC, and collagen protein families. Two peptides from three different protein families were combined serially in the proliferation assay, and the efficiency of the various peptide combinations was evaluated after calculating the isobolograms and combination index for each of the combinations. (*A*) The isobolograms for the combination of a TSP1 repeat-derived peptide and a collagen-derived peptide. (*B*) The isobolograms for the combination of a CXC- and a collagen-derived peptide. For each of the tested conditions (the individual peptides and the peptides tested in combination), proliferation dose response sigmoidal curves were estimated by fitting the data to sigmoidal Hill curves. Equally effective dose pairs in the combination experiments were then matched to the same level of inhibition obtained with a single peptide. The red highlighted areas designate peptide concentrations where the activity is synergistic, whereas the blue highlighted areas designate peptide concentrations where the activity is antagonistic.

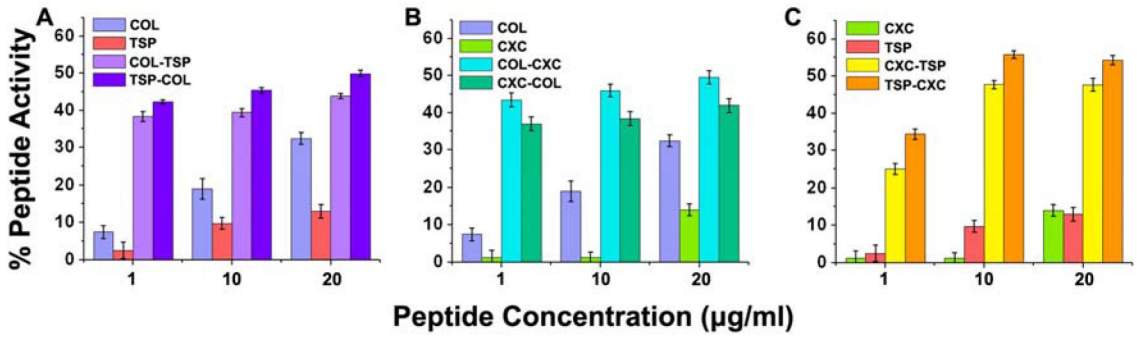

Fig. S6. The synergistic activity of the peptides when applied in combination is not significantly affected by the order in which the peptides are applied. (*A*) The activity in the proliferation assay of an α5 fibril of type IV collagen-derived peptide (pentastatin-1), and a TSP1-derived peptide (properdistatin) when applied alone, and in combination in a different order. (*B*) The activity in the proliferation assay of an α5 fibril of type IV collagen-derived peptide (pentastatin-1), and a CXC-derived peptide (chemokinostatin-1) when applied alone, and in combination with a different order. (*C*) The activity in the proliferation assay of a CXC-derived peptide (chemokinostatin-1) and a TSP1-derived peptide (properdistatin) when applied alone, and in combination with a different order.

Table S1. Query sequences, their location, the associated conserved domains they contain

Antiangiogenic protein	Location	Conserved domain
ADAMTS-1/METH-1	Q9UHI8(253–967)	TSP1
ADAMTS-8/METH-2	Q9UP79(215–890)	TSP1
Angiotensinogen	CAA33385(1–485)	Serpin
Antithrombin	AAA51796(1–464)	Serpin
Arresten	AAF72630(1–229)	CIV-CTR
BAI-1/Vasculostatin	NP_001693(31–880)	TSP1
BCA-1	CAG28552(1–109)	CXC
Calreticulin/Vasostatin	AAL13126(1–180)	
Canstatin	AAF72631(1–227)	CIV-CTR
Endorepelin/LG3	P98160(4201–4389)	Laminin G
Endostatin	AAH63833(1160–1330)	
Gro-beta	P19875(1–107)	CXC
Growth Hormone	CAA23779(1–134)	Somatotropin
Growth Hormone-tilted	CAA23779(101–114)	Somatotropin
IP-10	P02778(1–98)	CXC
ITAC	O14625(1–94)	CXC
K1	AAN85555(103–182)	Kringle
K2	AAN85555(185–262)	Kringle
K3	AAN85555(275–353)	Kringle
K4	AAN85555(377–455)	Kringle
K5	AAN85555(481–561)	Kringle
Kallistatin	AACIV1706(1–427)	Serpin
Kininogen D5 peptide	AAB59550(459–492)	
Kininostatin	AAB59550(438–531)	
Maspin	AAA18957(1–375)	Serpin
MIG	Q07325(1–125)	CXC
PEDF-34	AAA84914(44–77)	Serpin
PEDF-ERT	AAA84914(98–114)	Serpin
PEDF-TGA	AAA84914(36–46)	Serpin
PF4	AAI12094(78–101)	CXC
Placental Lactogen	AAA98621(1–134)	Somatotropin
Prolactin	CAA38264(1–132)	Somatotropin
Prolactin-tilted	CAA38264(101–114)	Somatotropin
Restin	CAI17044(1215–1381)	
TIMP2	AAB19474(171–194)	TIMP-NTR
TSP1/Mal2	NP_003237(442–460)	TSP1
TSP1/Mal3	NP_003237(499–517)	TSP1
Tumstatin/T3	AAF72632(69–88)	CIV-CTR
Tumstatin/T4	AAF72632(84–103)	CIV-CTR
Vastatin	AAH13581(581–744)	Complement C1q

Table S2. Identified similarity hits with respect to the proteins or protein fragments with known antiangiogenic activity

	80–100	60–80	40–60
PF-4		GCP-2/CXCL6 (AAH13744.1:86–109) ENA-78/CXCL5 (AAP35453.1:86–108) GRO-α/CXCL1 (AAP35526.1:80–103) THBG-β/CXCL7 (AAB46877.1:100–121)	GRO-β/CXCL2 (AAH15753.1:80–103) GRO-γ/MIP-2β/ CXCL3(AAA63184.1:79–100) IL-8/CXCL8 (AAP35730.1:72–94)
Timp2/loop 6		TIMP 4 (AAV38433.1:175–198)	TIMP 3 (AAA21815.1:148–171)
TSP1/Mal-II	TSP-2 (CAI23645.1:444–462)	THSD1 (AAQ88516.1:347–365) WISP-1 (AAH74841.1:221–238) BAI-2 (O60241:304–322) ADAMTS-16 (Q8TE57:1133–1149) CILP (AAQ89263.1:156–175) VSGP/F-spondin (BAB18461.1:621–639) BAI-3 (CAI21673.1:352–370) ADAMTS-18 (AAH63283.1:1131–1146) ADAMTS-2 (CAA05880.1:982–998) ADAMTS-3 (O15072.1:973–989) ADAMTS-9 (Q9P2N4:1247–1261) Semaphorin 5A (NP003957.1:848–866) TSRC1 (AAH27478.1:140–159) Fibulin-6 (CAC37630.1:1688–1706) CYR61 (AAR05446.1:234–251) ADAMTS-19 (Q8TE59:1096–1111) ADAMTS-12 (CAC20419.1:549–562) ADAMTS-20 (CAD56159.3:1661–1675) CTGF (CAC44023.1:204–221) ADAMTS-18 (AAH63283.1:998–1018) ADAMTS-7 (AAH61631.1:828–841)	Properdin (AAP43692.1:143–161) ADAMTS-9 (NP891550.1:595–613) ADAMTS-10 (Q9H324:528–546) ADAMTS-14 (CAI13857.1:980–994) ADAMTS-13 (AAQ88485.1:751–765) Papilin (NP775733.2:33–51) ADAMTS-1 (Q9UHI8:566–584) WISP-2 (AAQ89274.1:199–216) ADAMTS-4 (CAH72146.1:527–540) ADAMTS-6 (NP922932.2:847–860) ADAMTS-8 (Q9UP79:534–547) ADAMTS-20 (CAD56160.2:564–581) Semaphorin 5B (AAQ88491.1:916–934) WISP-3 (CAB16556.1:191–208) THSD6 (AAH40620.1:44–60) THSD3 (AAH33140.1:280–298) NOVH (AAL92490.1:211–228) C6 (AAB59433.1:30–48) UNC5D (AAQ88514.1:259–277) CILP-2 (AAN17826.1:153–171) ADAMTS-15 (Q8TE58:900–916) ADAMTS-5 (NP008969.1:882–898) UNC5C (AAH41156.1:267–285)
TSP1/Mal-III		ADAMTS-like 3 (NP_997400.1:425–442) Fibulin-6 (CAC37630.1:1574–1592) ADAMTS-18 (AAH63283.1:1131–1147) BAI-2 (O60241:304–322) TSP-2 (CAI23645.1:501–519) SCO-spondin (XP379967.2:3781–3799) ADAMTS-16 (Q8TE57:1133–1150) ADAMTS-12 (CAC20419:1479–1494) BAI-1 (O14514:361–379) ADAMTS-like 1 (NP443098.2:383–400) ADAMTS-16 (CAC86015.1:593–611) Semaphorin 5A (NP003957.1:660–678) ADAMTS-4 (CAH72146.1:527–545) ADAMTS-10 (Q9H324:528–546) Papilin (NP775733.2:342–359) BAI-3 (CAI21673.1:352–370) THSD1 (AAQ88516.1:347–365) ADAMTS-7 (AAH61631.1:1576–1592) ADAMTS-20 (CAD56159.3:1478–1494) ADAMTS-1 (Q9UHI8:566–584) CILP (AAQ89263.1:156–175) VSGP/F-spondin (BAB18461.1:567–583) ADAMTS-8 (Q9UP79:534–552) ADAMTS-6 (NP922932.2:847–863) UNC5D (AAQ88514.1:259–277) ADAMTS-9 (Q9P2N4:1335–1351) ADAMTS-18 (CAC83612.1:997–113)	Semaphorin 5B (AAQ88491.1: 731–747) VSGP/F-spondin (BAB18461.1:621–639) UNC5C (AAH41156.1:267–285) TSRC1 (AAH71852.1:140–156) Properdin (AAP43692.1:143–161) ADAMTS-20 (CAD56160.2:1309–1326) ADAMTS-7 (Q9UKP4:545–563) WISP-1 (AAH74841.1:221–237) ADAMTS-15 (Q8TE58:848–863) THSD3 (AAH33140.1:280–298) ADAMTS-17 (Q8TE56:928–945) ADAMTS-3 (O15072:973–989) ADAMTS-19 (Q8TE59:1096–1110) ADAMTS-14 (CAI13857.1:980–994) ADAMTS-13 (AAQ88485.1:751–765) TSRC1 (AAH27478.1:267–283) ADAMTS-like 2 (AAH50544.1:54–72) UNC5B (NP891550.1:595–613) ADAMTS-5 (NP008969.1:576–588) THSD6 (AAH40620.1:44–60) C6 (AAB59433.1:30–48) CILP-2 (AAN17826.1:153–171) CTGF (CAC44023.1:204–220) CYR61 (AAR05446.1:234–250) WISP-3 (CAB16556.1:191–207) WISP-2 (AAQ89274.1:199–215)
Tumstatin/Tum3	α5(CIV) (AAC27816.1:1510–1529) α1(CIV) (CAH74130.1:1494–1513)	α6(CIV) (CAI40758.1:1516–1535) α2(CIV) (P08572:1538–1557)	α4(CIV) (CAA56943.1:1514–1533)
Tumstatin/Tum4	α5(CIV) (AAC27816.1:1626–1644) α1(CIV) (CAH74130.1:1610–1628)	α2(CIV) (CAH71366.1:1646–1664) α6(CIV) (CAI40758.1:1630–1648) α4(CIV) (CAA56943.1:1628–1646)	ADAM-12 (O43184:662–674) ADAM-9 (Q13443:649–661)

	80–100	60–80	40–60
Growth Hormone Tilted		Placental Lactogen AAA98621(101–114) hGH-V AAB59548(101–114) Chorionic Somatomammotropin like 1 AAI19748(12–25) Transmembrane protein 45A NP_060474(181–194) Chorionic Somatomammotropin AAA52116(101–113)	Neuropeptide FF Receptor 2 Q9Y5X5(378–390) Brush border myosin 1 AAC27437(719–731) IL-17 receptor C Q8NAC3(376–387)
Angiostatin K1		Macrophage stim. 1 (AAH48330.1:368–448) Thrombin/cf II (AAL77436.1:106–186) HGF (P14210:127–206) Lp(a) (NP005568.1:4123–4201)	tPA (AAO34406.1:213–296) ROR-1 (CAH71706.1:312–392) ROR-2 (Q01974:315–394) KREMEN-1 (BAB40969.1:31–115) Hyaluronan binding (NP004123.1:192–276) Hageman fct/cf XII (AAM97932.1:215–296)
Angiostatin K2		HGF (P14210:304–383) Macrophage stim. 1 (AAH48330.1:188–268) Lp(a) (NP005568.1:3560–3639) AK-38 protein (AAK74187.1: 11–93)	ROR-1 (CAH71706.1:310–391) Thrombin/cf II (AAL77436.1:105–186) ROR-2 (Q01974:314–394) tPA (AAO34406.1:214–296) KREMEN-2 (BAD97142.1:35–119)
Angiostatin K3	Lp(a) (NP005568.1:1615–1690)	HGF (P14210:304–377) Macrophage stim. 1 (AAH48330.1:370–448)	AK-38 protein (AAK74187.1: 13–90) ROR-2 (Q01974:314–391) ROR-1 (CAH71706.1:311–388) Thrombin/cf II (AAL77436.1:107–183) Hageman fct/cf XII (AAM97932.1:216–292) KREMEN-1 (BAB40969.1:31–114) tPA (AAO3446.1.1:214–293)
Angiostatin K4	Lp(a) (NP005568.1:4225–4308)	HGF (P14210:304–383) AK-38 protein (AAK74187.1: 12–94) Macrophage stim. 1 (AAH48330.1:368–449) ROR-2 (Q01974:314–395)	ROR-1 (CAH71706.1:311–391) Thrombin/cf II (AAL77436.1:107–186) KREMEN-1 (BAB40969.1:31–114) tPA (AAO34406.1:213–297) Hageman fct/cf XII (AAM97932.1:214–295) Hyaluronan binding (NP004123.1:192–277)
Angiostatin K5	Lp(a) (NP005568.1:1615–1690) AK-38 protein (AAK74187.1: 14–93)	Macrophage stim. 1 (AAH48330.1:370–448)	HGF (P14210:127–207) tPA (AAM52248.1:5–89) Thrombin/cf II (AAL77436.1:105–186) ROR-2 (Q01974:315–395) ROR-1 (CAH71706.1:313–391) KREMEN-1 (BAB40969.1:31–114) KREMEN-2 (BAD97142.1:34–119) Hageman fct/cf XII (AAM97932.1:214–295)
Gro-β/CXCL2	GRO-γ/MIP-2β/CXCL3 (AAA63184.1:43–100) GRO-α/CXCL1 (AAP35526.1:44–101)	THBG-β/CXCL7 (AAB46877.1:64–121) ENA-78/CXCL5 (AAP35453.1:51–107)	GCP-2/CXCL6 (AAH13744.1:51–107) MIG/CXCL9 (Q07325:32–91) PF-4/CXCL4 (AAK29643.1:43–100) IL-8/CXCL8 (AAP35730.1:35–94)
IP-10/CXCL10			GCP-2/CXCL6 (AAH13744.1:47–106)
Kininogen			Hemopexin (P02790:233–246)
MIG/CXCL9			Gro-β/CXCL2 (AAH15753.1:42–97) GRO-γ/MIP-2β/ CXCL3(AAA63184.1:41–96) ENA-78/CXCL5 (AAP35453.1:48–103) GRO-α/CXCL1 (AAP35526.1:42–97) THBG-β/CXCL7 (AAB46877.1:62–117) IP-10/CXCL10 (AAH10954.1:29–86) GCP-2/CXCL6 (AAH13744.1:48–103)

Similarities with the antiangiogenic proteins or protein fragments of 20–60 amino acids (PF-4, TIMP-2/loop6, TSPs, Tums, PEDF-TGA, GH-tilted) and of 100–150 amino acids (angiostatin kringles, CXCs, and kininogen) were identified in a BLAST search against the human proteome. The results were filtered and similarities, based on a scaled score, of 80–100% are identified as ''identical,'' 60–80% as ''highly similar,'' and 45–60% as ''similar.'' The queries (first column) are listed alphabetically. The hits are displayed with their identification number and the corresponding part of their sequence that is identical. They are organized according to the degree of similarity with the query.

Table S3. The names and associated amino-acid sequences of the short antiangiogenic peptides

Peptide Name	Peptide Origin	Accession Number	Peptide Sequence
Collagen derived peptides			
Tetrastatin-1	α4 CIV	CAA56943(1514–1533)	LPVFSTLPFAYCNIHQVCHY
Tetrastatin-2	α4 CIV	CAA56943(1524–1543)	YCNIHQVCHYAQRNDRSYWL
Tetrastatin-3	α4 CIV	CAA56943(1628–1646)	AAPFLECQGRQGTCHFFAN
Pentastatin-1	α5 CIV	AAF66217(1516–1535)	LRRFSTMPFMFCNINNVCNF
Pentastatin-2	α5 CIV	AAF66217(1526–1545)	FCNINNVCNFASRNDYSYWL
Pentastatin-3	α5 CIV	AAF66217(1632–1650)	SAPFIECHGRGTCNYYANS
Hexastatin-1	α6 CIV	AAB19039(1629–1647)	ATPFIECSGARGTCHYFAN
Hexastatin-2	α6 CIV	AAB19039(1526–1545)	YCNINEVCHYARRNDKSYWL
Hexastatin-3	α6 CIV	AAB19039(1515–1534)	LPRFSTMPFIYCNINEVCHY
TSP-1 derived peptides			
Adamtsostatin-4	ADAMTS-4	AAD41494(527–545)	GPWGDCSRTCGGGVQFSSR
Adamtsostatin-16	ADAMTS-16	Q8TE57(1133–1149)	SPWSQCTASCGGGVQTR
Adamtsostatin-18	ADAMTS-18	CAC83612.1(595–613)	SKWSECSRTCGGGVKFQER
Adamtsostatin-like-4	TSRC1	Q6UY14(790–809)	SPWSQCSVRCGRGQRSRQVR
Cartilostatin-1	CILP-1	O75339(156–175)	SPWSKCSAACGQTGVQTRTR
Cartilostatin-2	CILP-2	Q8IUL8(153–171)	GPWGPCSGSCGPGRRLRRR
Cyrostatin	CYR61	O00622(234–251)	TSWSQCSKTCGTGISTRV
Complestatin-C6	Complement comp. C6	P13671(30–48)	TQWTSCSKTCNSGTQSRHR
Connectostatin	CTGF	P29279(204–221)	TEWSACSKTCGMGISTRV
Fibulostatin-6.1	Fibulin-6	Q96RW7(4536–4554)	SAWRACSVTCGKGIQKRSR
Fibulostatin-6.2	Fibulin-6	CAC37630.1(1745–1763)	ASWSACSVSCGGGARQRTR
Fibulostatin-6.3	Fibulin-6	CAC37630.1(1688–1706)	QPWGTCSESCGKGTQTRAR
Nephroblastostatin	NOVH	P48745(211–228)	TEWTACSKSCGMGFSTRV
Netrinstatin-5C	UNC-5C	O95185(267–285)	TEWSVCNSRCGRGYQKRTR
Netrinstatin-5D	UNC-5D	NP_543148.1(254–272)	TEWSACNVRCGRGWQKRSR
Papilostatin-1	Papilin	EAW81098.1(391–408)	GPWAPCSASCGGGSQSRS
Papilostatin-2	Papilin	EAW81098.1(33–51)	SQWSPCSRTCGGGVSFRER
Properdistatin	Properdin	AAB63280.1(143–161)	GPWEPCSVTCSKGTRTRRR
Scospondistatin	SCO-spondin	CAJ43920.1(3652–3670)	GPWEDCSVSCGGGEQLRSR
Semastatin-5A.1	Sema 5A	Q13591(660–678)	GPWERCTAQCGGGIQARRR
Semastatin-5A.2	Sema 5A	Q13591(848–866)	SPWTKCSATCGGGHYMRTR
Semastatin-5B	Sema 5B	AAQ88491.1(916–934)	TSWSPCSASCGGGHYQRTR
Spondinstatin-1	F-spondin	Q9HCB6(621–639)	SEWSDCSVTCGKGMRTRQR
Thrombostatin con-1	TSRC-1	Q9NS62(347–365)	QPWSQCSATCGDGVRERRR
Thrombostatin con-3	TSRC-3	AAI01021.1(333–351)	SPWSPCSGNCSTGKQQRTR
Thrombostatin con-6	TSRC-6	NP_998769(44–60)	WTRCSSSCGRGVSVRSR
Wispostatin-1	WISP-1	O95388(221–238)	SPWSPCSTSCGLGVSTRI
Wispostatin-2	WISP-2	O76076(199–216)	TAWGPCSTTCGLGMATRV
Wispostatin-3	WISP-3	Q8TE59(232–249)	TKWTPCSRTCGMGISNRV
CXC derived peptides			
Chemokinostatin-1	CXCL1/Gro-α	P09341(80–103)	NGRKACLNPASPIVKKIIEKMLNS
Chemokinostatin-3	CXCL3/Gro-γ	P19876(80–101)	NGKKACLNPASPMVQKIIEKIL
Chemokinostatin-5	CXCL5/ENA-78	P42830(86–108)	NGKEICLDPEAPFLKKVIQKILD
Chemokinostatin-6	CXCL6/GCP-2	P80162(86–109)	NGKQVCLDPEAPFLKKVIQKILDS
Chemokinostatin-7	CXCL7/PBP	P02775(100–121)	DGRKICLDPDAPRIKKIVQKKL
Chemokinostatin-8	CXCL8/IL-8	P10145(72–94)	DGRELCLDPKENWVQRVVEKFLK